IOPscience iopscience.iop.org

Home Search Collections Journals About Contact us My IOPscience

Lasing Behavior, Gain Property, and Strong Coupling Effects in GaN-Based Vertical-Cavity Surface-Emitting Lasers

This content has been downloaded from IOPscience. Please scroll down to see the full text.

2008 Jpn. J. Appl. Phys. 47 6655

(http://iopscience.iop.org/1347-4065/47/8S1/6655)

View the table of contents for this issue, or go to the journal homepage for more

Download details:

IP Address: 140.113.38.11
This content was downloaded on 25/04/2014 at 15:29

Please note that terms and conditions apply.

Japanese Journal of Applied Physics
Vol. 47, No. 8, 2008, pp. 6655–6659

Review Paper

©2008 The Japan Society of Applied Physics

Lasing Behavior, Gain Property, and Strong Coupling Effects in GaN-Based Vertical-Cavity Surface-Emitting Lasers

Tien-Chang LU, Jung-Tang CHU, Shih-Wei CHEN, Bo-Siao CHENG,
Hao-Chung KUO*, and Shing-Chung WANG

*Department of Photonics and Institute of Electro-Optical Engineering, National Chiao Tung University,
1001 Ta Hsueh Road, Hsinchu 300, Taiwan*

(Received February 18, 2008; accepted June 6, 2008; published online August 22, 2008)

The optical properties of a GaN-based vertical-cavity surface-emitting laser (VCSEL) with two dielectric distributed Bragg reflectors were investigated under optically pumped operation. The laser emits blue-violet light at a wavelength of 414 nm at room temperature with a high spontaneous emission coupling factor (β-factor) of 2×10^{-2} and a linewidth of 0.25 nm. The optical gain was determined by the Hakki–Paoli method by measuring the photoluminescence spectra below threshold conditions. At room temperature, an optical gain of 2900 cm^{-1} was obtained under threshold condition. The linewidth enhancement factor (α-factor) is estimated from the ratio of the wavelength and gain derivation with respect to the carrier density, and the α-factor at room temperature is estimated to be 2.8. Strong exciton-photon coupling in the microcavity was observed at room temperature. A 9 meV Rabi splitting with 60% peak-to-valley contrast was determined from the photoluminescence measurements. Emission spectra showing the evolution of anticrossing behavior were also observed.
[DOI: 10.1143/JJAP.47.6655]

KEYWORDS: InGaN, vertical-cavity surface-emitting lasers, gain, polariton

1. Introduction

GaN-based blue/violet vertical cavity surface-emitting lasers (VCSELs) have attracted much attention due to their many advantageous properties compared with edge emitting lasers, including circular beam shapes, light emission in the vertical direction, and two-dimensional arrays on the wafer level. A VCSEL structure consists of up by a microcavity a few wavelengths in length and a pair of high reflectivity (over 99%) distributed Bragg reflectors (DBRs) that are necessary to reduce the lasing threshold. Efforts to obtain optically pumped stimulated emission in GaN-based VCSELs have been reported by several groups. Someya *et al.*[1] and Zhou *et al.*[2] demonstrated lasing operation of VCSELs with structures of monolithically grown AlGaN/GaN DBRs, GaN/InGaN microcavities, and dielectric DBRs. GaN-based VCESLs with two dielectric DBRs were also proposed by Song *et al.*[3] and Tawara *et al.*[4] Our group has demonstrated initial lasing behavior in two types of GaN VCSELs: one with hybrid type DBRs which consist of a dielectric DBR and an epitaxially grown AlN/GaN DBR,[5] the other is a dielectric type VCSEL comprising a GaN active region and two dielectric DBRs.[6] In addition to lasing behavior in the GaN-based microcavity, the strong light-matter coupling in the semiconductor microcavity has attracted significant research activity[7–9] since the first demonstration of coupled exciton-photon mode splitting in a GaAs-based quantum microcavity was reported.[10] The strong interaction produces a quasiparticle state, cavity polariton, which has a vast potential in scientific and engineering applications, e.g., Bose–Einstein condensate, polariton lasers, and micro-optoelectronics. To realize such a device a microcavity is often used, which demands a material system with a significant exciton oscillator strength to counter linewidth broadening and a large binding energy for room temperature operation. Due to a large exciton binding energy and a large coupling with the light field compared to other III–V semiconductors, GaN-based materials are particularly promising for the realization of cavity polaritons at room temperature, and a few promising experiments have demonstrated despite the challenges presented by crystal growth and inhomogeneous broadening.[11,12)]

In this paper, we report the laser emission and gain properties of GaN-based VCSELs with InGaN/GaN multiple quantum wells (MQWs) and two dielectric DBRs during optically pumped operation at room temperature. The laser emission properties showed a dependence of the emission spectrum on pumping energy. A high spontaneous emission factor was obtained. The optical gain was determined by the Hakki–Paoli[13] method by measuring the photoluminescence (PL) spectra below threshold conditions. The linewidth enhancement factor (α-factor) estimated from the ratio of the wavelength and gain derivation with respect to the carrier density was determined. Cavity polaritons were observed in the VCSEL structure. A 9 meV Rabi splitting with large peak-to-valley contrast as high as 60% from the microcavity was observed from PL emissions at room temperature. Emission spectra showing the evolution of anticrossing behavior were also observed. Indium inhomogeneity in the InGaN/GaN MQWs was verified by cathode luminescence (CL) measurement. The relation between strong coupling in the microcavity and In inhomogeneity is discussed.

2. Experimental Methods

The VCSEL layer structure grown on a (0001)-oriented sapphire substrate by metal-organic chemical vapor deposition (MOCVD) included: a 30-nm GaN nucleation layer, a 4-µm GaN bulk layer, MQWs consisting of 10 periods of 5-nm GaN barriers and 3-nm $In_{0.1}Ga_{0.9}N$ wells, and a 200-nm GaN cap layer. A six-pair layer of alternating SiO_2 and TiO_2 was evaporated on the top of the VCSEL structure to form the first dielectric DBR. The maximum reflectivity of the SiO_2/TiO_2 DBR is 99%. Next, an array of circular SiO_2/TiO_2 DBR mesas with diameters of 60 µm was formed by lithography and chemical wet etching. To deposit the second

*E-mail address: hckuo@faculty.nctu.edu.tw

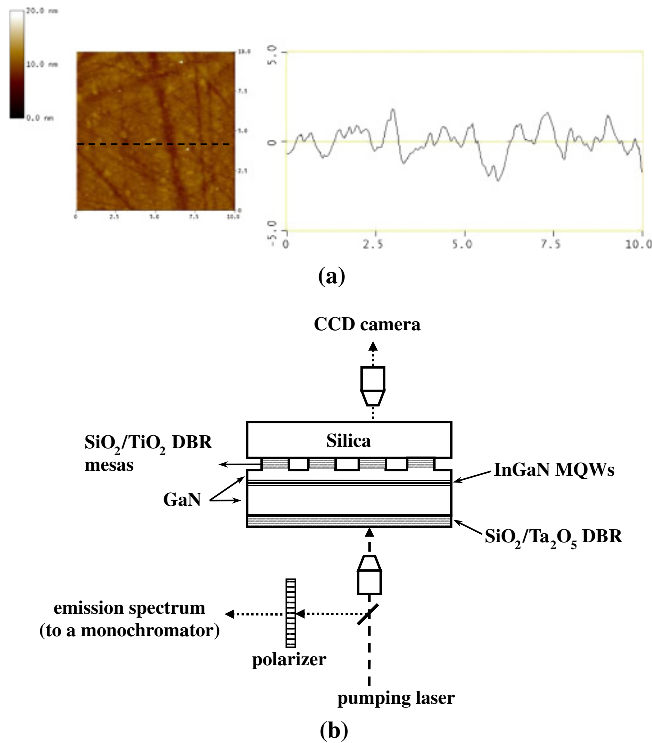

Fig. 1. (Color online) (a) In-plane AFM image and cross-sectional profile of the polished GaN surface after LLO. (b) Schematic GaN-based VCSEL structure and measurement setup.

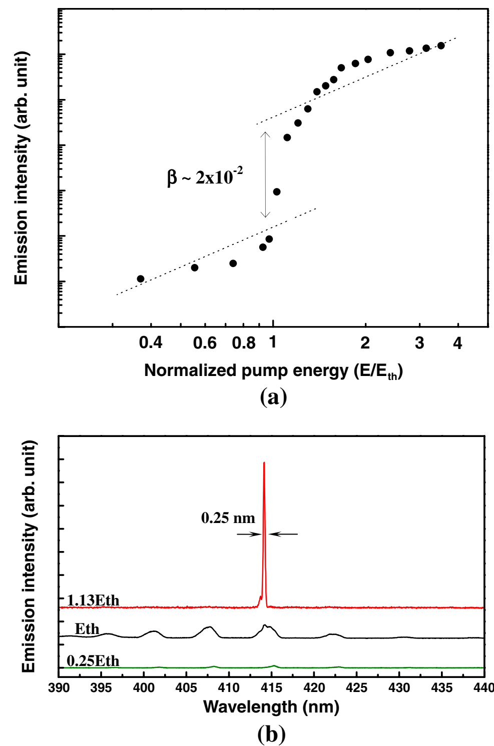

Fig. 2. (Color online) (a) Laser emission intensity versus pumping energy on logarithmic scale. The β value estimated from the difference between the two dashed lines is approximately 2×10^{-2}. (b) Emission spectra from the GaN-VCSEL at various pumping energies. The lasing emission wavelength is 414 nm with a linewidth of 0.25 nm.

dielectric DBR, the structure was subjected to laser lift-off (LLO) using a KrF excimer laser to remove the sapphire substrate. In the next step, the sample was lapped and polished using diamond powder to smooth the GaN surface, because the LLO left a roughened surface. Figure 1(a) shows the in-plane atomic force microscopy (AFM) image and the cross-sectional profile of the polished GaN surface. The mean roughness of the surface was approximately 1 nm over a scanned area of $10 \times 10\,\mu m^2$. In order to reduce the decrease in reflectance of the DBRs due to optical scattering, it is important to smooth the surface where the DBRs are deposited. However, to prevent the possible degradation of the quality of MQWs during lapping, a GaN bulk layer about 4 µm in thickness was preserved. Finally, a second DBR consisting of eight pairs of SiO_2 and Ta_2O_5 layers was evaporation-deposited on the polished GaN surface. The Ta_2O_5 was used to reduce the absorption of the pumping beam at a wavelength of 355 nm. The maximum reflectivity of the SiO_2/Ta_2O_5 DBR is 98%. For the detailed process procedure, please refer to our previous report.[6]

Figure 1(b) shows the schematic VCSEL structure and measurement setup. The fabricated GaN-based VCSELs were optically pumped by a Nd:YVO4 laser at 355 nm, with a repetition rate of 1 KHz and a pulse width of 0.5 ns. The pumping laser beam with a focused spot size approximately 40 µm in diameter was vertically incident on the VCSEL sample from the SiO_2/Ta_2O_5 DBR side. The light emission from the VCSEL sample was collected by an imaging optic into a spectrometer with a spectral resolution of 0.05 nm. The polarizer was used to measure the polarization of the laser emission from the VCSELs. In the polariton measurement, a *cw* He-Cd laser at 325 nm was used as the pumping source in the same measurement setup. The focused spot size on the MQWs layer in the microcavity is estimated to be 1.5 µm in diameter.

3. Results and Discussion

3.1 Lasing behavior

The laser emission intensity as a function of normalized pumping energy is shown in Fig. 2(a) on a logarithmic scale. Clear evidence of threshold behavior was observed at a pumping energy density of $E_{th} = 21.5\,mJ/cm^2$. From the logarithmic data, the spontaneous emission factor, which indicated the coupling efficiency of the spontaneous emission to the lasing mode, can be estimated from the difference between the heights of the emission intensities before and after lasing. The factor is estimated to be about 2×10^{-2}, which agrees with the reported result[4] and is nearly three orders of magnitude higher than that of typical GaN edge-emitting semiconductor lasers,[1] indicating the enhancement of the spontaneous emission into a lasing mode by the high cavity quality factor of the microcavity in the VCSEL structure. In our previous report,[14] multiple lasing spot emissions inside an aperture were observed. This observation indicates that the effective cavity volume of the lasing mode is the volume of the spot emission, not the volume of the aperture. Therefore, the large spontaneous emission factor obtained in our VCSEL structure could contribute to the "small" cavity volume of the spot lasing mode. Figure 2(b) shows the evolution of the VCSEL emission spectrum as a function of the pumping energy at room temperature. When the pumping energy is below the threshold, the spontaneous emission spectrum shows multi-

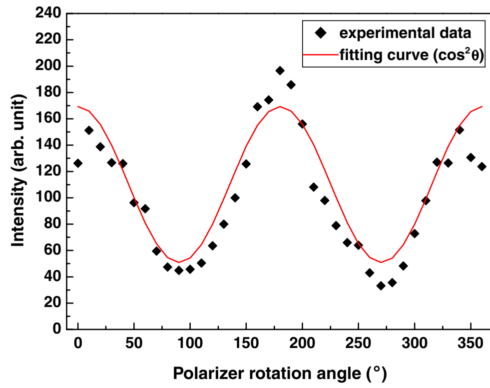

Fig. 3. (Color online) Polarization characteristics of the VCSEL. The degree of polarization is calculated to be 70%.

ple cavity modes. As pumping energy increases above the threshold, a dominant laser emission line appears at 414 nm with a narrow linewidth of approximately 0.25 nm. The lasing wavelength is located at one of the cavity modes near the peak emission wavelength of the InGaN MQWs.

Figure 3 shows the laser emission intensity as a function of the angle of the polarizer at a pumping energy of $1.3E_{th}$. The variation in the laser emission intensity with the angle of the polarizer is nearly a cosine square variation. The degree of polarization (P) is defined as $P = (I_{max} - I_{min})/(I_{max} + I_{min})$, where I_{max} and I_{min} are the maximum and minimum intensity variations, respectively, as the polarizer is rotated. The solid line in the figure was fit to the experimental data in accordance with a cosine square equation. The result shows that the laser beam has a degree of polarization of about 70%, suggesting a near-linear polarization of the laser emission.

3.2 *Gain measurement*

As shown in Fig. 2(b), several cavity modes are shown in the PL spectra when the pumping energy is below the lasing threshold. The gain spectrum of the InGaN/GaN MQWs can therefore be evaluated by the Hakki–Paoli method which determines the spectral gain from the modulation depth of the Fabry–Perot modes in the amplified spontaneous emission spectra below the laser threshold. By applying the Hakki–Paoli method, the material gain in our VCSEL structure can be expressed as:

$$G(\lambda) = \frac{\Gamma}{d_a} \ln\left[\frac{(I^+)^{1/2} + (I^-)^{1/2}}{(I^+)^{1/2} - (I^-)^{1/2}}\right] - \left(\frac{1}{2d_a}\right) \ln(R_1 R_2) + \frac{\alpha L}{d_a}, \quad (1)$$

where λ is the wavelength at which the cavity modes are being measured, the confinement factor of the laser structure is $\Gamma = 0.05$, d_a is the thickness of the 10 quantum wells, the cavity mode maximum and minimum intensities are I^+ and I^-, respectively DBR reflectivities R_1 and R_2 are 99 and 98%, respectively, the average absorption coefficient is $\alpha = 30\,\text{cm}^{-1}$, and the cavity length $L = 4\,\mu\text{m}$. With eq. (1), the individual optical gain for each cavity mode under different pumping levels can be obtained. The gain spectra of the VCSEL under different pumping levels at room temperature are shown in Fig. 4(a). The wavelength of each

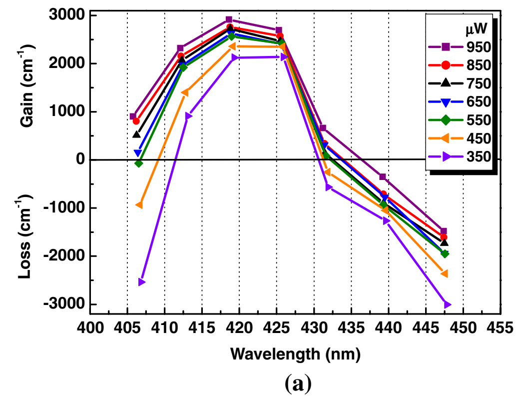

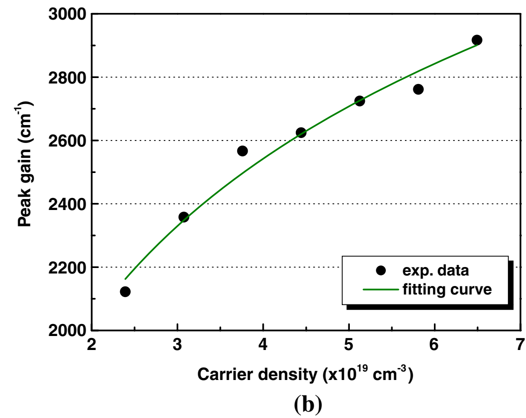

Fig. 4. (Color online) (a) The gain spectrum of the VCSEL under different pumping levels at room temperature. (b) The dependence of the material peak gain on pumping carrier density. The solid curves were fit to the measured data according to eq. (2).

cavity mode shows a slight blue-shift due to the decreasing refractive index of the MQWs layer as the pumping power increases, as a result of the deviation of the carrier density and gain. In Fig. 4(b) the dependence of the peak material gain of the lasing mode on pumping carrier density is shown. Here, the carrier density in QWs is estimated from the energy density of the pumping laser, assuming that the pumping light with an emission wavelength of 355 nm has experienced a 60% transmission through the SiO_2/Ta_2O_5 DBR layers and has undergone a 98% absorption in the thick GaN layer with an absorption coefficient of $104\,\text{cm}^{-1}$.[15] For increasing carrier density, rising material gains are observed and follow the logarithmic law expressing the relationship between gain and carrier density in QWs,[16]

$$g(N) = g_0 \ln\left(\frac{N}{N_0}\right), \quad (2)$$

where g_0 is a constant describing the increasing rate of gain corresponding to increasing carrier density, N is the carrier density in the MQWs, and N_0 is the transparent carrier density. The solid curve in Fig. 4(b) was fit to the measured data according to eq. (2). At the threshold condition the peak optical gain is about $2900\,\text{cm}^{-1}$, which is in agreement with reported results.[17,18] According to the fitting result, g_0 and N_0 are $740\,\text{cm}^{-1}$ and $1.3 \times 10^{18}\,\text{cm}^{-3}$, respectively. In comparison with the transparent carrier density of $9.3 \times 10^{19}\,\text{cm}^{-3}$ in the GaN-based edge emitting laser report by Nakamura,[18] the lower transparent carrier density may be due to the MQWs with superior crystal quality in our

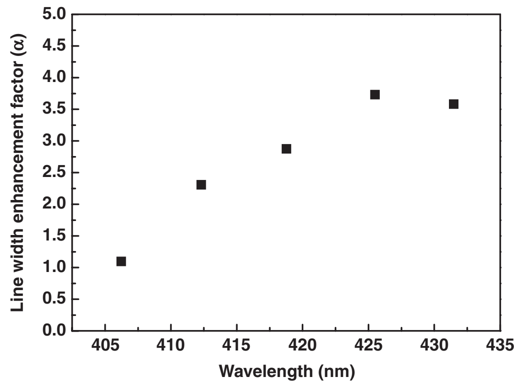

Fig. 5. Calculated α-factor as a function of wavelength.

VCSEL structure. Nonuniform indium composition in the MQWs could be another possible reason for the low transparent carrier density obtained in our VCSEL structure. As mentioned previously, the spot laser emission due to indium inhomogeneity in the MQWs was observed in our VCSEL structure. We believe the local indium inhomogeneity would cause energy fluctuations in the band diagram in the MQWs. The energy fluctuations therefore induce carrier redistribution and spatially nonuniform distribution of optical gain. The indium inhomogeneity in InGaN MQWs is considered to be a dot-like region.[19,20] The dot-like regions could contribute to the observation of relatively low transparent carrier density in our VCSEL structure.

The linewidth enhancement factor can be measured from the amplified spontaneous emission spectra below the threshold condition by the following method.[21] The α-factor is the ratio of the change in the refractive index (n) with carrier density (N) with respect to the change in optical gain with carrier density. This can be expressed as

$$\alpha = -\frac{4\pi}{\lambda}\frac{dn/dN}{dg/dN}, \quad (3)$$

where λ is the wavelength of light. Using eq. (3), the α-factor can be calculated from the emission spectra at different pumping levels below the threshold. The change in refractive index was determined from the wavelength shift $d\lambda$ of the cavity mode according to the relationship

$$dn = \frac{\lambda}{2L\Delta\lambda}d\lambda, \quad (4)$$

where $\Delta\lambda$ is the cavity mode spacing, L is the cavity length, and $d\lambda$ is the wavelength shift when the carrier density is varied by dN.

Substituting eqs. (1) and (4) into eq. (3) and canceling out the carrier density term, the α-factor can be obtained,

$$\alpha = \frac{2\pi}{L\Delta\lambda}\frac{d\lambda}{dg}, \quad (5)$$

where dg is the change in optical gain as the carrier is changed by dN.

The calculated α-factors as a function of wavelength are shown in Fig. 5. The α-factors depend on wavelength and are small at shorter wavelengths. For the lasing mode, the α-factor was estimated to be 2.8 and is in agreement with the reported data for GaN-based edge emitting laser.[22]

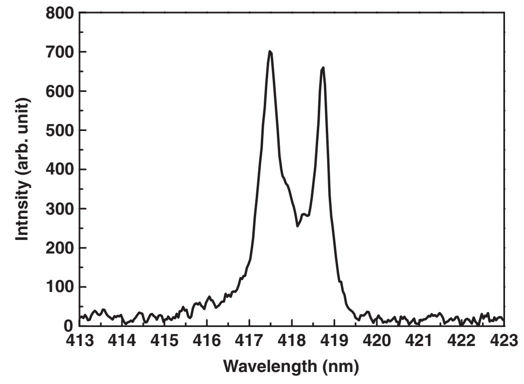

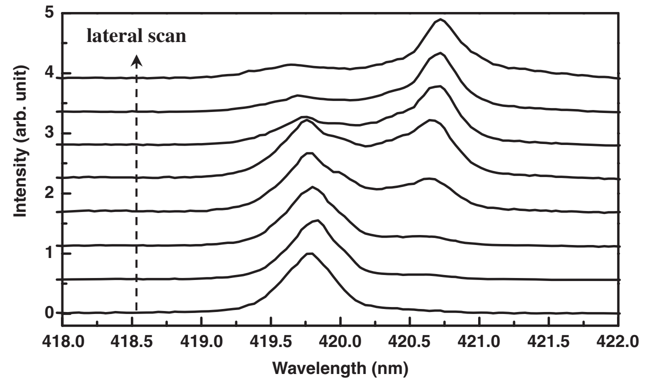

Fig. 6. (a) Rabi splitting with 60% peak-to-valley contrast and 9 meV. (b) PL spectra as the pumping location is scanned laterally in 2-μm steps.

3.3 Strong coupling effect

A typical PL spectrum shows a linewidth of 0.3 nm in our microcavity structure. A cavity quality factor (Q-factor) can be expressed as $\lambda/\Delta\lambda$, where λ is the PL wavelength and $\Delta\lambda$ is the linewidth of the PL spectrum. The Q-factor can therefore be estimated as approximately 1400 in our microcavity structure. This value implies that the GaN-based cavities provide a high Q-factor for the strong coupling between the photon and exciton modes. In the measurement, we scanned and measured PL spectra over the aperture (inside SiO_2/TiO_2 DBR mesa). The mode-splitting PL can be observed in specific locations inside the aperture. Figure 6(a) shows a mode-splitting PL with a 9 meV Rabi splitting and 60% peak-to-valley contrast. The large and clear splitting at room temperature is noticeable in the GaN-based microcavity. Because of the lateral variations in layer thickness and InGaN concentration due to the growth and subsequent processes, the exciton and cavity resonant frequencies match only at specific locations. We scanned along a straight line passing through the location with mode-splitting PL. Figure 6(b) shows the evolution of PL spectra along a straight line in 2-μm steps. At first, one peak appeared; as the laser spot moved, the second peak appeared, and then the first peak disappeared, leaving the second peak. The evolution of the spectra shows a smooth transition of anticrossing, implying a variation from positive cavity detuning to negative cavity detuning as the laser spot moves along the straight line. The anticrossing behavior could be due to energy bandgap fluctuation in the MQWs causing positive or negative cavity detuning between the exciton and cavity modes.

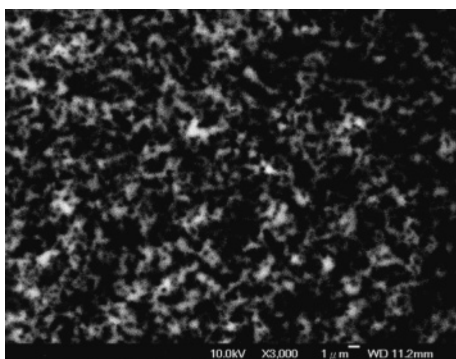

Fig. 7. The monochromatic CL in-plane map of the as-grown InGaN MQWs sample at 410 nm.

To further investigate the indium inhomogeneity in our InGaN MQWs, the as-grown cavity with InGaN MQWs used in the microcavity structure was examined. Figure 7 shows a monochromatic CL in-plane map of the as-grown InGaN MQWs sample at 410 nm. The image shows that the nonuniform CL emission intensity has patches of bright areas approximately 1–2 μm in size. The spatially nonuniform emission intensity implies indium inhomogeneity in the MQWs and consequently results in slight energy bandgap fluctuations in a local area. Thus, as the pump laser moved across the local energy bandgap fluctuation area, the evolution of cavity detuning from positive to negative was observed.

4. Conclusions

In summary, the optical characteristics of a GaN-based VCSEL with two dielectric DBRs were investigated under optical pumping at room temperature. The laser emits blue-violet light at a wavelength of 414 nm with a high spontaneous emission coupling factor of 2×10^{-2} and a linewidth of 0.25 nm. The optical gain was determined by the Hakki–Paoli method by measuring the photoluminescence spectra below threshold conditions. At room temperature, an optical gain of 2900 cm^{-1} was obtained under threshold conditions. The α-factor, estimated by a ratio of the wavelength and gain derivation with respect to the carrier density is 2.8 at room temperature. Strong exciton-photon coupling in the InGaN MQWs microcavity was observed at room temperature. Strong exciton-photon coupling in the microcavity was observed at room temperature. A 9 meV Rabi splitting with 60% peak-to-valley contrast was determined from photoluminescence measurements. Emission spectra showing the evolution of anticrossing behavior were also observed.

Acknowledgments

This work was supported by the MOE ATU program and in part by the National Science Council of Taiwan under contracts NSC-96-2120-M-009-006 and NSC-96-2221-E-009-067.

1) T. Someya, R. Werner, A. Forchel, M. Catalano, R. Cingolani, and Y. Arakawa: Science **285** (1999) 1905.
2) H. Zhou, M. Diagne, E. Makarona, A. V. Nurmikko, J. Han, K. E. Waldrip, and J. J. Figiel: Electron. Lett. **36** (2000) 1777.
3) Y. K. Song, H. Zhou, M. Diagne, A. V. Nurmikko, R. P. Schneider, Jr., C. P. Cuo, M. R. Krames, R. S. Kern, C. Carter-Coman, and F. A. Kish: Appl. Phys. Lett. **76** (2000) 1662.
4) T. Tawara, H. Gotoh, T. Akasaka, N. Kobayashi, and T. Saitoh: Appl. Phys. Lett. **83** (2003) 830.
5) C. C. Kao, Y. C. Peng, H. H. Yao, J. Y. Tsai, Y. H. Chang, J. T. Chu, H. W. Huang, T. T. Kao, T. C. Lu, H. C. Kuo, and S. C. Wang: Appl. Phys. Lett. **87** (2005) 081105.
6) J. T. Chu, T. C. Lu, H. H. Yao, C. C. Kao, W. D. Liang, J. Y. Tsai, H. C. Kuo, and S. C. Wang: Jpn. J. Appl. Phys. **45** (2006) 2556.
7) R. Houdre, C. Weisbuch, R. P. Stanley, U. Oesterle, P. Pellandini, and M. Ilegems: Phys. Rev. Lett. **73** (1994) 2043.
8) J. P. Reithmaier, G. Sek, A. Loffler, C. Hofmann, S. Kuhn, S. Reitzenstein, L. V. Keldysh, V. D. Kulakovskii, T. L. Reinecke, and A. Forchel: Nature **432** (2004) 197.
9) H. Deng, G. Weihs, C. Santori, J. Bloch, and Y. Yamamoto: Science **298** (2002) 199.
10) C. Weisbuch, M. Nishioka, A. Ishikawa, and Y. Arakawa: Phys. Rev. Lett. **69** (1992) 3314.
11) T. Tawara, H. Gotoh, T. Akasaka, N. Kobayashi, and T. Saitoh: Phys. Rev. Lett. **92** (2004) 256402.
12) E. Feltin, G. Christmann, R. Butté, J.-F. Carlin, M. Mosca, and N. Grandjean: Appl. Phys. Lett. **89** (2006) 071107.
13) B. W. Hakki and T. L. Paoli: J. Appl. Phys. **44** (1973) 4113.
14) J. T. Chu, T. C. Lu, M. You, B. J. Su, C. C. Kao, H. C. Kuo, and S. C. Wang: Appl. Phys. Lett. **89** (2006) 121112.
15) M. O. Manasreh: Phys. Rev. B **53** (1996) 16425.
16) T. Makino: IEEE J. Quantum Electron. **32** (1996) 493.
17) Y.-K. Song, M. Kuball, and A. V. Nurmikko: Appl. Phys. Lett. **72** (1998) 1418.
18) S. Nakamura: IEEE J. Sel. Top. Quantum Electron. **3** (1997) 712.
19) Y. Narukawa, Y. Kawakami, M. Funato, S. Fujita, S. Fujita, and S. Nakamura: Appl. Phys. Lett. **70** (1997) 981.
20) Y. T. Moon, D. J. Kim, J. S. Park, J. T. Oh, J. M. Lee, Y. W. Ok, H. S. Kim, and S. J. Park: Appl. Phys. Lett. **79** (2001) 599.
21) I. D. Henning and J. V. Collines: Electron. Lett. **19** (1983) 972.
22) U. T. Schwarz, E. Sturm, and W. Wegscheider: Appl. Phys. Lett. **83** (2003) 4095.